HHS Public Access

Author manuscript

Aquat Toxicol. Author manuscript; available in PMC 2020 January 14.

Published in final edited form as:

Aquat Toxicol. 2018 January ; 194: 185–194. doi:10.1016/j.aquatox.2017.11.017.

Uptake, tissue distribution, and toxicity of polystyrene nanoparticles in developing zebrafish (*Danio rerio*)

Jordan A. Pitt[1,2,*], **Jordan S. Kozal**[1], **Nishad Jayasundara**[1,3], **Andrey Massarsky**[1], **Rafael Trevisan**[1], **Nick Geitner**[4], **Mark Wiesner**[4], **Edward D. Levin**[5], **Richard T. Di Giulio**[1]

[1]Nicholas School of the Environment, Duke University, Durham, NC 27708, USA.

[2]College of Environmental Science and Forestry, State University of New York, Syracuse, NY 13210, USA.

[3]School of Marine Sciences, University of Maine, Orono, ME, 04469, USA

[4]Department of Civil and Environmental Engineering and the Center for the Environmental Implications of Nano Technology, Durham, NC 27708, USA

[5]Department of Psychiatry and Behavioral Sciences, Duke University Medical Center, Durham, NC 27710, USA

Abstract

Plastic pollution is a critical environmental concern and comprises the majority of anthropogenic debris in the ocean, including macro, micro, and likely nano-scale (less than 100 nm in at least one dimension) plastic particles. While the toxicity of macroplastics and microplastics is relatively well studied, the toxicity of nanoplastics is largely uncharacterized. Here, fluorescent polystyrene nanoparticles (PS NPs) were used to investigate the potential toxicity of nanoplastics in developing zebrafish (*Danio rerio*), as well as characterize the uptake and distribution of the particles within embryos and larvae. Zebrafish embryos at 6 h post-fertilization (hpf) were exposed to PS NPs (0.1, 1, or 10 ppm) until 120 hpf. Our results demonstrate that PS NPs accumulated in the yolk sac as early as 24 hpf and migrated to the gastrointestinal tract, gallbladder, liver, pancreas, heart, and brain throughout development (48 hpf-120 hpf). Accumulation of PS NPs decreased during the depuration phase (120 hpf-168 hpf) in all organs, but at a slower rate in the pancreas and gastrointestinal tract. Notably, exposure to PS NPs did not induce significant mortality, deformities, or changes to mitochondrial bioenergetics, but did decrease the heart rate. Lastly, exposure to PS NPs altered larval behavior as evidenced by swimming hypoactivity in exposed larvae. Taken together, these data suggest that at least some nanoplastics can penetrate the chorion

[*]**Corresponding author**: jopitt@syr.edu.

Author Contributions

Jordan S. Kozal and Nishad Jayasundara conceived and designed the experiments. Jordan A. Pitt, Jordan S. Kozal, Andrey Massarsky, and Rafael Trevisan performed the exposures and toxicity endpoints. Andrey Massarsky imaged the larvae. Rafael Trevisan and Nick Geitner characterized the polystyrene nanoparticles. Jordan A. Pitt, Jordan S. Kozal, and Edward D. Levin analyzed the data. Richard T. Di Giulio, Edward D. Levin, and Mark Wiesner provided reagents, analytical tools, and testing facilities. Richard T. Di Giulio supervised the project and provided conceptual advice. Jordan A. Pitt wrote the paper. Jordan S. Kozal, Nishad Jayasundara, Andrey Massarsky, Rafael Trevisan, Nick Geitner, and Richard T. Di Giulio edited the manuscript. All authors have read and approved of the manuscript.

Declaration of Interests

The authors have no competing interests.

of developing zebrafish, accumulate in the tissues, and affect physiology and behavior, potentially affecting organismal fitness in contaminated aquatic ecosystems.

Keywords

Behavioral changes; Cardiotoxicity; Plastic pollution; Polystyrene nanoparticles; Uptake and accumulation; Zebrafish (*Danio rerio*)

1. Introduction

Plastics are ubiquitous in aquatic environments, accounting for 50–80% of marine debris (Barnes et al., 2009). While the hazard of macroplastics is well studied, the degradation of macroplastic debris in the ocean and the beach litter into microplastics and nanoplastics has recently become a significant concern and an increasingly important area of research (Andrady, 2011). In fact, while macroplastics are the most widely studied, microplastics and nanoplastics may actually be more pervasive by number in marine environments (Cózar et al., 2014). They also can have a great effect through the food web chain: microplastics have been found to accumulate in zooplankton (Cole et al., 2013), and nanoplastics have been shown to pass from algae to zooplankton and fish (Mattsson et al., 2015a).

Nanoplastics are the least well-studied form of plastic debris, with little known about their environmental concentrations, bioaccumulation potential, or toxicity. Nanoplastics are defined as plastic particles having at least one dimension in the nanoscale (1–100 nm) (Andrady, 2011; Mattsson et al., 2015b). Nanoplastics are hypothesized to be abundant in aquatic environments due to the deficit of plastic at the lower end of the expected particle size distribution (Cózar et al., 2014). The abundance of nanoplastics is likely due to physical and photo-degradation of macro and microplastics in the environment (Andrady, 2011). However, nanoplastics have yet to be quantified in natural systems, because the necessary analytical methods are still under development (Koelmans, 2015).

The biological effects of nanoplastics remain understudied (Rios and Moore, 2007). Most toxicological studies on nanomaterials have focused on metal and carbon based nanoparticles, while very little is known about the toxicity of nanoplastics, such as polystyrene nanoparticles (PS NPs). Polystyrene (PS) is one of the most abundant forms of plastic debris found in the marine environment. For example, PS was the second most common form of floating plastic debris by number found at Tamar Estuary in Southwest England, constituting 25% of the debris (polyethylene was the most common form at 40%) (Sadri and Thompson, 2014). In adult fish, exposure to PS NPs has been shown to compromise immune responses in fathead minnows (*Pimephales promelas*) (Greven et al., 2016) and induce liver lesions in zebrafish (*Danio rerio*) (Lu et al., 2016). Carboxylated PS NPs have been shown to accumulate in the gut of various marine organisms, such as sea urchin embryos (*Paracentrotus lividus*) and brine shrimp (*Artemia fanciscana*), and as a result it is hypothesized that PS NPs can bio-magnify via trophic transfer (Bergami et al., 2016; Della Torre et al., 2014). Further, it has been demonstrated that PS NPs that accumulate in algae (*Scenedesmus* sp.) can be passed up the food chain and ultimately affect behavior, physiology, and metabolism of Crucian Carp (*Carassius carassius*) (Mattsson et al.,

2015a). Thus, fish in the environment are likely exposed to nanoplastics directly through ingestion and through the gills, as well as indirectly via trophic transfer within the food chain (Lu et al., 2016; Mattson et al., 2014).

All of the aforementioned studies focused on the toxicity of PS NPs to adult life stages of fish and other aquatic organisms. In contrast, relatively few studies have focused on the effects of PS NPs on developmental life stages of fish. PS NPs have previously been shown to penetrate the chorion of Japanese medaka (*Oryzias latipes*) embryos (Manabe et al., 2011). However, van Pomeren et al. (2017) reported that PS NPs did not pass through the chorion of developing zebrafish, though oral exposure played a major role on PS NPs uptake. Additionally, Veneman et al. (2017) reported that injection of PS particles (700 nm) into the yolk sac of 2-day old zebrafish resulted not only in particle distribution throughout the bloodstream and accumulation in the heart region, but also in upregulation of the immunological response, characterized by presence of neutrophils and macrophages around PS particles.

To this end, the present study aimed to assess the potential bioaccumulation and toxicity of PS NPs in embryonic and early larval stages of zebrafish. We predicted that the PS NPs would pass through the zebrafish chorion since the particles are smaller than the pore size (0.6–0.7 μm) and were shown to penetrate the chorion of medaka (Kirsten, 2011; Manabe et al., 2011). Further, we hypothesized that PS NPs would accumulate in various regions, including yolk sac, pericardium, gallbladder, and gut, similarly to previous studies (Manabe et al., 2011; Skjolding et al., 2017; Veneman et al., 2017). Finally, given that PS NPs have been shown to accumulate at multiple tissues throughout the development, we predicted that PS NPs could alter zebrafish physiology, bioenergetics, and behavior (Chen et al. 2017, Mattson et al. 2014).

2. Materials and methods

2.1 PS NPs

PS NPs (cat. #FSDG001) were purchased from Bangs Laboratories, Inc. (Fishers, IN, USA). The stock solution contained 1% fluorescent (internally labeled with Dragon Green; ex./em. 480/520) PS NPs with a nominal mean diameter of 51 nm. According to the manufacturer, internal labeling does not change the particle surface chemistry, and thus should not affect their adsorptive and bioaccumulative properties. Additionally, the stock solution contained up to 0.1% sodium dodecyl sulfate (SDS) and 0.09% sodium azide. An aliquot of stock solution was sonicated for 60 s at 50/60 Hz using NEY Ultrasonic Cleaner ULTASONIK 2QT/H (Barkmeyer Division Yucaipa, Ca, USA) prior to preparation of the working solutions (see section 2.4).

2.2. PS NPs characterization

PS NPs were characterized using a dynamic light scattering (DLS) (Zetasizer Nano, Malvern Instruments Ltd., Malvern, UK). The hydrodynamic diameter and zeta potential of 5 ppm PS NPs were assessed in the exposure medium (see section 2.4).

2.3. Zebrafish husbandry and embryo collection

Laboratory reared wild-type (EkkWill Waterlife Resources; Ruskin, FL) *D. rerio* were maintained in a recirculating AHAB system (Aquatic Habitats, Inc., Apopka, FL, USA) on a 14:10 h light/dark cycle. Water quality was maintained at 28–29°C, pH 7.0–7.5, and 60 ppm artificial seawater (ASW; Instant Ocean, Foster & Smith, Rhinelander, WI, USA). The fish were fed twice daily with brine shrimp (INVE Aquaculture, Inc., Salt Lake City, UT, USA) in the morning and Zeigler's Adult Zebrafish Complete Diet (Aquatic Habitats, Inc.) in the afternoon. Breeding crosses (3 females: 2 males) were set at 5 PM, and embryos were collected the following morning within 1 h of spawning between 9 and 10 AM and kept in 30% Danieau's medium (17.4 mM NaCl, 0.21 mM KCl, 0.12 mM $MgSO_4$, 0.18 mM $Ca(NO_3)_2$, and 1.5 mM HEPES at pH 7.6) at 28°C. All zebrafish care and husbandry procedures were approved by the Duke University Institutional Animal Care and Use Committee (A139-16-06).

2.4. Experimental set-up

At 6 h post-fertilization (hpf), embryos were randomly assigned to 20 mL glass scintillation vials with 2 embryos per vial. Each vial contained 7.5 mL of 65 ppm ASW supplemented with 0.00003% methylene blue. The 65 ppm ASW medium used is similar to zebrafish egg water established by Westerfield (2000). The embryos were randomly sorted into 4 groups: 0 (control), 0.1, 1, and 10 ppm PS NPs; these concentrations are up to 2 orders of magnitude lower than the concentrations used in a previous zebrafish embryo study (van Pomeren et al., 2017). The vials also contained 0.0001% SDS and 0.00009% sodium azide for the 10 ppm PS NPs solution with decreasing orders of magnitude for the 1 and 0.1 ppm solutions from the stock PS NPs solution (SDS and sodium azide are included in the stock solution to prevent aggregation and bacterial growth, respectively). Such concentrations of SDS and sodium azide did not significantly affect mortality, hatching success, heart rate, pericardial area, and uptake of PS NPs. Inclusion of methylene blue also did not significantly affect the toxicity of PS NPs (see sections 1 and 2 of Supplemental Materials for details). The embryos/larvae were exposed to PS NPs until 120 hpf without refreshing the exposure medium. Observations continued from 120 hpf until 168 hpf in 65 ppm ASW medium without PS NPs in order to assess the relative amount of PS NPs after the exposure. The toxicity endpoints were repeated using at least 3 independent zebrafish cohorts (see details below).

2.5. General physiology

Survival rate was assessed daily from 24 to 120 hpf, and dead organisms were removed. A total of 240 embryos were used per group. Hatching rate was assessed at 72 hpf by the inspection of a total of 50 embryos per group. Both the survival and hatching rates were calculated from at least 3 independent experiments (n=3–8), which were based on cohorts from separate breeding events. Heart rate was measured at 72 hpf using tricaine as an anesthetic agent [125 mg/L in 30% Danieau's medium; a concentration shown not to have a notable effect on embryonic heart rate (Huang et al., 2010)]. The larvae were washed and placed into the tricaine solution for 5 min. Following this, heart rate was individually evaluated by counting beats for 15 sec in 5 randomly selected larvae from different vials in

each treatment group in 3 cohorts from separate breeding events (n=15). Larval deformities were analyzed using bright field images that were taken during the fluorescence imaging of the larvae (see section 2.6). Deformities were analyzed at 24 h intervals from 48 hpf to 168 hpf. At every time point, 5 individuals from each treatment group were imaged (n=5). Specifically, presence or absence of spinal curvature and craniofacial abnormality were assessed in a blind fashion. Pericardial area was quantified in 5 larvae per treatment group (n=5) at 72 hpf using ImageJ software (National Institutes of Health, Bethesda, MD, USA).

2.6. Uptake and distribution of PS NPs

Zebrafish were imaged using Zeiss Axioskop (Carl Zeiss, Oberkochen, Germany) at 24 h intervals from 24 hpf to 168 hpf. At every time point, 5 randomly selected individuals from each treatment group were imaged (n=5). While the zebrafish were exposed with their chorions intact, the 24 hpf embryos were imaged both pre and post enzymatic dechorionation with pronase (1 mg/mL). Fluorescence images were captured using a 75W/2 xenon short-arc lamp, a Photometric CoolSNAPfx monochromne CCD camera (Roper Scientific, Tuscon, AR, USA), 480/30 nm (emission) and 535/40 nm (ex) filters, and 100 ms camera exposure. Organ placement in the larvae was analyzed using illustrations from Wallace and Pack (2003). Fluorescence intensity was analyzed using ImageJ software. The brightness/contrast of fluorescent images was adjusted to the brightness/contrast of the fluorescent signal corresponding to 10 ppm PS NPs. The fluorescence values were normalized to the control group and expressed as fold change. Due to the high difference in fluorescence levels between the exposure groups (up to 250 fold), log transformed values were used in the statistical analysis.

2.7. Larval behavior

At 120 hpf, zebrafish larvae were washed and transferred into beakers with 200 mL of fresh media. The larvae were transported to the behavioral testing facilities, where they were kept on a 14:10 h light/dark cycle at 28 °C. At 144 hpf, around 12 pm, the larvae were transferred into a 96 well plate (1 larvae/well, 23–24 wells/treatment group, in 3 cohorts from separate breeding events, n=70–72). The larvae were allowed to acclimate for an hour in the dark, prior to being transferred to a DanioVision™ observation chamber (Noldus Inc., Wageningen, The Netherlands) for an alternating light/dark test (Massarsky et al., 2015; Brown et al., 2016; Bailey et al., 2016). This is a 50 minute test where the first 10 minute period is habituation in the dark, and then the subsequent 40 minutes consist of 2 cycles of alternating 10 minute periods of light and dark. Video data were recorded at a sample rate of 30 times/second via a high-speed infrared camera. The EthoVision XT® software (Noldus, Wageningen, The Netherlands) was used to calculate total distance moved for each individual larvae throughout the test.

2.8 Bioenergetics

The oxygen consumption rate (OCR) was assessed using the XFe24 Extracellular Flux Analyzer (Agilent Instruments, CA, USA). This bioenergetic profiling method was adapted from Stackley et al. (2011). For this assessment, embryos (24 hpf) were staged in a 24 well plate with 700 μL of 65 ppm artificial seawater (2 embryos/well, 5 wells/exposure group, 4 blank wells). Carbonyl cyanide 4-(trifluoromethoxy) phenylhydrazone (FCCP) and sodium

azide were loaded into separate injection ports, resulting in working concentrations of 2.5 μM and 6.25 mM in the well, respectively. The plate was then inserted into the Analyzer where 8 OCR measurements (basal OCR) were first taken before the FCCP was injected into the wells (8 measurements) followed by the sodium azide injections (25 measurements). The FCCP acts as a mitochondrial un-coupler allowing for measurement of maximal respiration, and the sodium azide inhibits cyctochrome c oxidase function allowing for measurement of non-mitochondrial respiration. The total basal OCR was calculated by averaging the three lowest values from the basal measurements. The OCR in the presence of pharmaceutical agents was calculated by averaging the three highest values for the FCCP treatment (total maximal) and by averaging the three lowest values for the sodium azide treatment (non-mitochondrial). These OCR measurements were used to calculate additional respiratory parameters, including basal mitochondrial, maximal mitochondrial, and mitochondrial reserve capacity. The extracellular acidification rate (ECAR) was detected concurrently with the OCR measurements. This parameter is used as a proxy for glycolytic activity. This allowed for the calculation of the total basal ECAR and OCR/ECAR values, which estimates the degree to which the embryo utilizes oxidative phosphorylation versus glycolytic activity.

2.9. Statistical analysis

For fluorescence imaging and deformity endpoints, one-way or two-way Analysis of Variance (ANOVA) with a Fisher's LSD post hoc method were used to assess statistical differences among treatment groups. Such analyses were carried out with log transformed values for fluorescence endpoints. For heart rate, two-way ANOVA with treatment and cohort factors with a Fisher's LSD post hoc method was used to test for PS NPs treatment effects. These analyses were conducted using Graph Pad Prism 6.0 (San Diego, CA, USA). For larval behavior, mixed-design repeated-measures ANOVA with treatment group and cohort as the between-subject factors and light condition and trial minute as the repeated measures was used with a Dunnett's two-tailed post hoc to test for PS NPs treatment effects. This analysis was conducted using StatView 5.0.1 (SAS Institute, Cary, NC). For all endpoints, p-value <0.05 was considered statistically significant.

3. Results

3.1. PS NPs characterization

The PS NPs (5 ppm in ASW medium) ranged from 20 to 100 nm in diameter with a mean hydrodynamic diameter of 34.5±10.8 nm. The zeta potential was −21.1±2.47 mV. Both values indicate a low aggregation behavior for these PS NPs.

3.2. General physiology

Mortality was not significantly different between the exposure groups throughout embryonic and larval development at any of the time points measured (24–120 hpf) (Fig. 1A). The hatching success was also not significantly different between exposure groups (Fig. 1A). Exposure to PS NPs did not induce deformities nor did it increase the pericardial area (Fig. 1B). In contrast, heart rate was significantly decreased in larvae from all exposure groups relative to control (Fig. 1C). Specifically, heart rate decreased in a dose-dependent manner

by 5%, 8%, and 10% in the 0.1, 1, and 10 ppm PS NPs treatment groups relative to controls, respectively.

3.3. Uptake and distribution of PS NPs

Green fluorescence was used to qualitatively and quantitatively evaluate uptake and distribution of PS NPs in zebrafish embryos and early larval stages between 24 hpf to 168 hpf. At 24 hpf, fluorescence was mainly observed in 1 and 10 ppm PS NPs exposed embryos in the yolk sac with some fluorescence also observed in the head in the 10 ppm group (Fig. 2). Aggregation of the PS NPs was visible on the surface of the chorions of some exposed embryos (Fig. 2A). At 24 hpf, the fluorescence of the yolk sac region was significantly higher in zebrafish embryos exposed to 1 and 10 ppm PS NPs relative to the control (11 and 102 fold higher, respectively) (Fig. 2C).

At 48 hpf and 72 hpf, the fluorescence levels were significantly higher in the yolk sac and head (presumably the brain) even at the lowest concentration (Fig. S3 & S4). At these same time points, fluorescence was also strongly observed in the pericardium at 1 and 10 ppm PS NPs (Fig. S3 & S4).

By 120 hpf, the larva has resorbed the yolk sac, and the gastrointestinal (GI) tract is functional. At this stage in larval development, fluorescence was higher in the GI tract, pancreas, and the head for all the exposure groups relative to controls. At 1 ppm and 10 ppm PS NPs, fluorescence was also higher in the liver, gall bladder, and pericardium (Fig. 3). The magnitude of the fluorescence in the GI tract and the pancreas appeared to be relatively constant after removal of the larvae from the exposure medium (144 hpf – Fig. S5, and 168 hpf – Fig. 4); however, the fluorescence in the head, gall bladder, liver, and pericardium began to decrease in all exposure groups during the depuration. Despite the decrease, the fluorescence levels in all the tissues analyzed from larvae exposed to 10 ppm PS NPs remained significantly higher than those of the controls (Fig. S5, Fig. 4). Fluorescence levels remained significantly higher in the GI tract and pancreas in larvae exposed to 1 ppm PS NPs, and they returned to control values in all the analyzed organs in the lowest exposure group (Fig. S5, Fig. 4).

The fluorescence values of each analyzed tissue during the exposure and depuration periods are summarized in Figure 5. PS NPs quickly accumulate in the yolk sac, head, and pericardium by 48 hpf, with the highest fluorescence levels in the pericardium. Between 72 and 120 hpf, fluorescence levels start to decrease in these organs, a possible sign of PS NPs excretion. During the depuration period (144–168 hpf), fluorescence levels continue to decrease in the head and pericardium, as well as gall bladder and liver. As previously mentioned, fluorescence levels remain stable and significantly higher than controls in the GI tract and pancreas only at 1 and 10 ppm PS NPs.

3.4. Larval behavior

Larval locomotor activity over the course of an alternating light/dark test was measured at 144 hpf, following a 24 h acclimation in clean embryo medium. PS NPs exposure significantly reduced larval locomotor activity (Fig. 6). Specifically, there was a significant main effect of PS NPs treatment on total distance traveled over the course of the alternating

light-dark test. This effect was driven by significant hypoactivity in larvae from the medium (1 ppm) PS NPs group ($p<0.05$) relative to control throughout the trial (Dunnett's two-tailed post hoc test). As expected, there was a significant main effect of light condition ($p<0.0001$) on locomotor activity, with larvae from all treatments swimming more in the dark than the light. There was not a significant interaction of light condition and PS NPs treatment ($p<0.98$). However, while significant hypoactivity relative to control was measured in the 1 ppm PS NPs exposed larvae during the initial habituation period in the dark ($p<0.05$) and the alternating dark periods ($p<0.02$), this effect was trending but not significant in the alternating light periods ($p<0.11$) (Fig. 6A & B). While not significant, the larvae exposed to 0.1 or 10 ppm PS NPs also appeared to be hypoactive relative to the control group. Notably, there were significant interactions of PS NPs treatment and cohort during both the acclimation period ($p<0.02$) and the alternating light-dark test ($p<0.04$), reducing the interpretability of these data.

3.4. Bioenergetics

The basal, maximal, and non-mitochondrial OCR values were not significantly different across treatment groups. The calculated values for basal mitochondrial, maximal mitochondrial, and mitochondrial reserve were also not different. No significant differences were noted for ECAR or the ratio of basal OCR to ECAR (Fig. S6).

4. Discussion

While the hazards associated with macro and microplastics to aquatic organisms are relatively well characterized, the bioaccumulation and toxicity of nanoplastics are only beginning to be considered even though they could potentially be more hazardous (Koelmans, 2015). The current study provides strong evidence that PS NPs are taken up by developing zebrafish, localize to specific tissues, and potentially exert toxic effects that are suggested by their tissue localization pattern. The following sections discuss our results in detail and consider the potential physiological and ecological implications associated with exposure to PS NPs, which are likely a ubiquitous contaminant in aquatic environments.

First, we demonstrate that PS NPs are able to penetrate the zebrafish chorion, which is a known physical barrier to some chemicals (Mizell and Romig, 1997). The PS NPs initially accumulate in the yolk sac and the head, and later in other regions, including pericardium, gall bladder, pancreas, liver and GI tract. These results are consistent with the findings of analogous studies in medaka (Manabe et al., 2011; Kashiwada, 2006), but are in contrast with those of van Pomeren et al. (2017), who reported that the chorion was an effective barrier against PS NPs. These discrepancies are likely due to differences in PS NPs concentration (our study used lower concentrations), supplier (and/or synthesis method) of the PS NPs, and the size of the particles [in our study the particles were approximately half the size of those used by van Pomeren et al. (2017)]. The ability of PS NPs to penetrate the chorion suggests that accumulation in aquatic environments could affect development of fish species and potentially have long lasting impacts at the population level.

While nanoparticles have a tendency to aggregate and PS NPs aggregates were occasionally observed on the outside of the chorion, there was high fluorescence visible within the yolk

sacs of the dechorionated embryos as early as 24 hpf. This suggests that the chorion may act as a barrier against PS NPs aggregates but does not exclude PS NPs at the studied size (34.5 nm mean diameter). Further, the yolk sac appears to be a main target during the initial PS NPs uptake. The yolk sac is the nutrient reserve for the developing zebrafish, containing lipids that are processed and mobilized by lipoproteins and are essential for metabolic and developmental processes (Fraher et al., 2016). PS NPs have been shown to interact with lipid membranes (Rossi et al., 2014), and PS microparticles have been shown to alter lipid metabolism and induce hepatic lipid accumulation in zebrafish (Lu et al., 2016). Notably, multiple nuclear receptors involved in lipid metabolism are upregulated following microinjection of 700 nm PS particles into the yolk sac of zebrafish (Veneman et al., 2017). Early life exposure to PS seems to affect lipid metabolism in zebrafish, which could indicate that PS NPs have the potential to induce metabolic disorders. It is also possible that the high lipid content of the yolk sac could be a target for PS NPs accumulation, where further lipid mobilization could play a role on the distribution of PS NPs throughout the embryo/larva.

Despite the apparent ability of PS NPs to penetrate the chorion, PS NPs had no effect on mortality, hatching success, deformities, or pericardial area. However, zebrafish exposed to PS NPs exhibited significant bradycardia. Notably zebrafish from all exposure groups (0.1, 1, and 10 ppm) had significantly reduced heart rates relative to controls, suggesting that changes in heart function occur even at relatively low PS NPs concentrations. A number of factors may play a role in reduced heart rates. One possibility is that PS NPs may interact with cardiac sarcomeres. Previous findings suggest that PS NPs are localized into cells and are not membrane bound (Geiser et al., 2005) creating potential for interactions with cardiac sarcomeres affecting heart rate. Another possibility is that oxidative stress is occurring, as suggested previously (Chen et al. 2017), altering the function of the heart. Future studies will be necessary to determine the mechanism by which PS NPs reduce heart rate. PS NPs-induced bradycardia may have negative implications for fish in the aquatic ecosystems where cardiac function and aerobic condition may influence predator prey interactions and other factors important for organismal ecological fitness.

Further, the present study is the first to show that PS NPs also localize to the GI tract, heart, head, liver, and pancreas as the zebrafish develops and the yolk sac is resorbed. Fluorescence was detected even at the lowest PS NPs concentration (at the ppb range), highlighting the potential bioaccumulation of these compounds throughout the fish development. It is important to highlight that the fluorescence intensities detected here may actually underestimate the amount of PS NPs in the developing zebrafish due to increased pigmentation and skull development that occurs during the time frame studied. The presence of PS NPs in the GI tract is in agreement with the findings of Skjolding et al. (2017) and Van Pomeren et al. (2017), and PS NPs presence in the pericardium was also noted by Veneman et al. (2017). Most notably for this study, PS NPs were shown to localize in the pericardium only at 1 ppm and 10 ppm, but a significant decrease in the heart rate was observed even in larvae exposed to 0.1 ppm PS NPs. This suggests that even a low concentration of PS NPs is enough to observe cardiotoxicity. Moreover, the degree of fluorescence intensities decreased over time in all affected organs when the larvae were removed from the exposure media. The fluorescence observed in the 10 ppm PS NPs group was still significant after two days of depuration, but it returned to values similar to the control in lower concentrations. The high

and constant fluorescence levels in the GI tract during depuration indicate at least two possible scenarios. The GI tract may be an important site for PS NPs excretion, which is consistent with excretion route of carbon-based nanoparticles (Zhao et al., 2014). Alternatively, the clearance rate of PS NPs adsorbed within the intestinal tract is very slow, potentially impeding its function.

Significant PS NP fluorescence was also detected in the head, presumably the brain, of the zebrafish. This finding is consistent with previous studies that found PS NPs in brain tissues of fish exposed directly or through an aquatic food chain (Kashiwada, 2006; Mattsson et al., 2015a), suggesting that PS NPs are capable of penetrating the blood-brain barrier (Mattsson et al., 2017). PS NPs can translocate into red blood cells and are not membrane bound (Geiser et al., 2005), and therefore could enter the brain circulated via the blood. As the blood-brain barrier is established at approximately 72 hpf in zebrafish (Xie et al., 2010), and PS NPs were detected at significant fluorescence levels in the head of the embryos as soon as 24 hpf and 48 hpf, it could be expected that there is a larger PS NP uptake by the brain at early stages. After the blood-brain barrier is formed at 72 hpf, PS NPs fluorescence sharply decreases over time, suggesting that the faster clearance at later stages could be due to the formation of the blood-brain barrier. However, it has been previously shown that 53 nm PS NPs can pass through the blood-brain barrier (Mattsson et al., 2017). Thus, the role of the blood-barrier formation in the uptake of PS NPs should be examined in more details in future studies.

Given that PS NPs were shown to localize in the head (thus possibly the brain) as early as 24 hpf and throughout subsequent development, larval locomotor activity was evaluated to assess the potential of these nanoparticles to disrupt neural development and ultimately behavior. Zebrafish larvae exposed to PS NPs were hypoactive relative to controls over the course of an alternating light/dark test. This effect was driven by significantly reduced locomotor activity in the 1 ppm exposure group. Although this observation suggests that hypoactivity could be due to neurological differences rather than a mobility issue, the metabolic effects of PS NPs could not be excluded. While our OCR data suggests that there was no impact of PS NPs on mitochondrial function at 24 hpf, metabolic effects could occur later on due to a prolonged PS NPs exposure. Future studies should examine this issue on more details. It is noteworthy that decreased activity as well as altered feeding and shoaling behaviors have previously been shown in adult Crucian Carp (*Carassius carassius*) exposed to PS NPs through an aquatic food chain (Mattsson et al. 2015a, Mattsson et al., 2017). It is possible that the PS NPs are triggering a specific targeting mechanism within the brain; however, further studies will be required to elucidate the precise mechanisms by which PS NPs exposure affects locomotor activity in early developmental stages. These findings are consistent with the hypoactivity observed by Chen et al. (2017), who suggested that PS NPs-induced hypoactivity is due to oxidative stress and reduced acetylcholinesterase activity. In an aquatic ecosystem, PS NPs-induced hypoactivity could reduce organismal fitness by affecting foraging or predator avoidance behaviors. While we show functional effects on heart and brain tissues herein, future studies will be necessary to determine whether there are functional effects on other tissue types where PS NPs accumulate.

The lack of mortality, morphological deformities, and normal mitochondrial metabolism suggest that PS NPs exposure would not result in acute lethal toxicity in wild fish populations. However, behavioral and cardiac effects could become pervasive throughout the fish populations. Specifically, both of these effects could reduce organismal ecological fitness, such as decreased ability to avoid predation, which could ultimately lead to decreased biodiversity in wild populations. It is also possible that the PS NPs could affect reproductive fitness or even cause transgenerational effects as PS NPs have been found to accumulate in the testes of zebrafish (Kashiwada, 2006). Future work should also examine how presence of nanoplastics can alter the effects of chemical, physical, and/or biological stressors, since aquatic organisms often face multiple stressors simultaneously.

In summary, the present study revealed that PS NPs can penetrate the zebrafish chorion and are taken up by the embryo. PS NPs initially localize to the yolk sac, but the particles migrate to the pericardium, head, pancreas, gallbladder, liver, and GI tract throughout development, even in the ppb range of exposure. Significant physiological effects of PS NPs exposure (e.g. bradycardia and hypoactivity) were quantified in tissues where the particles were shown to localize (e.g. pericardium and head, respectively), including at low exposure levels. Further, PS NPs exposures in the ppm range did not result in significant mortality or morphological deformities, suggesting that the observed toxic effects were not secondary to teratogenesis. Together these data suggest that PS NPs may induce organ toxicity specific to their developmental distribution pattern.

Supplementary Material

Refer to Web version on PubMed Central for supplementary material.

Acknowledgements

We thank all the members of the Di Giulio laboratory for help with zebrafish husbandry. We highly appreciate the technical assistance of Dr. Stella Marinakos during nanoparticle characterization and Dr. Lilah Glazer during locomotor assessment. We also thank the Center for the Environmental Implications of Nanotechnology's Research Experience for Undergraduates Program and Dr. Glenda Kelly, the REU program coordinator. Research was supported by Duke's Superfund Research Center (NIEHS P42-ES010356), Duke's Program in Environmental Health (ITEHP) Training Grant (NIEHS T32-ES021432), and Duke's Center for the Environmental Implications of Nanotechnology (NSF 3331894).

5. References

Andrady AL (2011). Microplastics in the marine environment. Marine pollution bulletin, 62(8), 1596–1605. [PubMed: 21742351]

Bailey JM, Oliveri AN, Karbhari N, Brooks RA, Amberlene J, Janardhan S, Levin ED (2016). Persistent behavioral effects following early life exposure to retinoic acid or valproic acid in zebrafish. Neurotoxicology, 52, 23–33. [PubMed: 26439099]

Bar-Ilan O, Louis KM, Yang SP, Pedersen JA, Hamers RJ, Peterson RE, and Heideman W (2012) Titanium dioxide nanoparticles produce phototoxicity in the developing zebrafish. Nanotoxicology 6, 670–679. [PubMed: 21830861]

Barnes DK, Galgani F, Thompson RC, & Barlaz M (2009). Accumulation and fragmentation of plastic debris in global environments. Philosophical Transactions of the Royal Society B: Biological Sciences, 364(1526), 1985–1998.

Bergami E, Bocci E, Vannuccini ML, Monopoli M, Salvati A, Dawson KA, & Corsi I (2016). Nano-sized polystyrene affects feeding, behavior and physiology of brine shrimp Artemia franciscana

larvae. Ecotoxicology and Environmental Safety, 123, 18–25. doi:10.1016/j.ecoenv.2015.09.021 [PubMed: 26422775]

Brown DR, Bailey JM, Oliveri AN, Levin ED, & Di Giulio RT (2016). Developmental exposure to a complex PAH mixture causes persistent behavioral effects in naive Fundulus heteroclitus (killifish) but not in a population of PAH-adapted killifish. Neurotoxicology and Teratology, 53, 55–63. [PubMed: 26548404]

Canesi L, Ciacci C, Fabbri R, Balbi T, Salis A, Damonte G, & Corsi I (2016). Interactions of cationic polystyrene nanoparticles with marine bivalve hemocytes in a physiological environment: Role of soluble hemolymph proteins. Environmental Research, 150, 73–81. doi:10.1016/j.envres.2016.05.045 [PubMed: 27257827]

Chen Q, Gundlach M, Yang S, Jiang J, Velki M, Yin D, & Hollert H (2017). Quantitative investigation of the mechanisms of microplastics and nanoplastics toward zebrafish larvae locomotor activity. Science of The Total Environment, 584–585, 1022–1031. doi:10.1016/j.scitotenv.2017.01.156

Cole M, Lindeque P, Fileman E, Halsband C, Goodhead R, Moger J, & Galloway TS (2013). Microplastic Ingestion by Zooplankton. Environmental Science & Technology Environ. Sci. Technol, 47(12), 6646–6655. doi: 10.1021/es400663f [PubMed: 23692270]

Cózar A, Echevarría F, Ignacio González-Gordillo J, Irigoien X, Úbeda B, Hernández-León S, et al. (2014). Plastic debris in the open ocean. Proceedings of the National Academy of Sciences, 111(28), 10239–10244.

Della Torre CD, Bergami E, Salvati A, Faleri C, Cirino P, Dawson KA, & Corsi I (2014). Accumulation and Embryotoxicity of Polystyrene Nanoparticles at Early Stage of Development of Sea Urchin Embryos Paracentrotus lividus. Environmental Science & Technology 48(20), 12302–12311. doi: 10.1021/es502569w [PubMed: 25260196]

Fraher D, Sanigorski A, Mellett NA, Meikle PJ, Sinclair AJ, & Gibert Y (2016). Zebrafish embryonic lipidomic analysis reveals that the yolk cell is metabolically active in processing lipid. Cell reports, 14(6), 1317–1329. [PubMed: 26854233]

Geiser M, Rothen-Rutishauser B, Kapp N, Schürch S, Kreyling W, Schulz H, & Gehr P (2005). Ultrafine Particles Cross Cellular Membranes by Nonphagocytic Mechanisms in Lungs and in Cultured Cells. Environmental Health Perspectives,113(11), 1555–1560. [PubMed: 16263511]

Greven AC, Merk T, Karagöz F, Mohr K, Klapper M, Jovanović B, & Palić D (2016). Polycarbonate and polystyrene nanoplastic particles act as stressors to the innate immune system of fathead minnow (*Pimephales promelas*). Environmental toxicology and chemistry, 35(12), 3093–3100. [PubMed: 27207313]

Henn K (2011). Limits of the fish embryo toxicity test with Danio rerio as an alternative to the acute fish toxicity test (Doctoral dissertation).

Huang WC, Hsieh YS, Chen IH, Wang CH, Chang HW, Yang CC, & Chuang YJ (2010). Combined use of MS-222 (tricaine) and isoflurane extends anesthesia time and minimizes cardiac rhythm side effects in adult zebrafish. Zebrafish, 7(3), 297–304. [PubMed: 20807039]

Kashiwada S (2006). Distribution of nanoparticles in the see-through medaka (*Oryzias latipes*). Environmental health perspectives, 114(11), 1697. [PubMed: 17107855]

Koelmans AA, Besseling E, & Shim WJ (2015). Nanoplastics in the aquatic environment. Critical review In Marine anthropogenic litter (pp. 325–340). Springer International Publishing.

Lu Y, Zhang Y, Deng Y, Jiang W, Zhao Y, Geng J, & Ren H (2016). Uptake and accumulation of polystyrene microplastics in zebrafish (*Danio rerio*) and toxic effects in liver. Environmental Science & Technology, 50(7), 4054–4060. [PubMed: 26950772]

Manabe M, Tatarazako N, & Kinoshita M (2011). Uptake, excretion and toxicity of nano-sized latex particles on medaka (*Oryzias latipes*) embryos and larvae. Aquatic Toxicology, 105(3), 576–581. [PubMed: 21946167]

Massarsky A, Jayasundara N, Bailey JM, Oliveri AN, Levin ED, Prasad GL, & Di Giulio RT (2015). Teratogenic, bioenergetic, and behavioral effects of exposure to total particulate matter on early development of zebrafish (*Danio rerio*) are not mimicked by nicotine. Neurotoxicology and Teratology, 51, 77–88. [PubMed: 26391568]

Mattsson K, Ekvall MT, Hansson LA, Linse S, Malmendal A, & Cedervall T (2015a). Altered behavior, physiology, and metabolism in fish exposed to polystyrene nanoparticles. Environmental Science & Technology, 49(1), 553–561. [PubMed: 25380515]

Mattsson K, Hansson LA, & Cedervall T (2015b). Nano-plastics in the aquatic environment. Environmental Science: Processes & Impacts, 17(10), 1712–1721. [PubMed: 26337600]

Mattsson K, Johnson EV, Malmendal A, Linse S, Hansson LA, & Cedervall T (2017). Brain damage and behavioural disorders in fish induced by plastic nanoparticles delivered through the food chain. Scientific Reports, 7(1), 11452. [PubMed: 28904346]

Mizell M, Romig ES (1997). The aquatic vertebrate embryo as a sentinel for toxins: zebrafish embryo dechorionation and perivitelline space microinjection. Int. J. Dev. Biol 41, 411–423. [PubMed: 9184351]

Rios LM, Moore C, & Jones PR (2007). Persistent organic pollutants carried by synthetic polymers in the ocean environment. Marine Pollution Bulletin, 54(8), 1230–1237. [PubMed: 17532349]

Rossi G, Barnoud J, & Monticelli L (2013). Polystyrene nanoparticles perturb lipid membranes. The journal of physical chemistry letters, 5(1), 241–246. [PubMed: 26276207]

Sadri SS, & Thompson RC (2014). On the quantity and composition of floating plastic debris entering and leaving the Tamar Estuary, Southwest England. Marine Pollution Bulletin, 81(1), 55–60. [PubMed: 24613232]

Skjolding LM, Ašmonaitė G, Jølck RI, Andresen TL, Selck H, Baun A, & Sturve J (2017). An assessment of the importance of exposure routes to the uptake and internal localization of fluorescent nanoparticles in zebrafish (Danio rerio), using light sheet microscopy. Nanotoxicology, 11(3), 351–359. [PubMed: 28286999]

Stackley KD, et al. (2011). Bioenergetic profiling of zebrafish embryonic development. PLoS One, 6(9): p. e25652. [PubMed: 21980518]

van Pomeren M, Brun NR, Peijnenburg WJGM, & Vijver MG (2017). Exploring uptake and biodistribution of polystyrene (nano) particles in zebrafish embryos at different developmental stages. Aquatic Toxicology, 190, 40–45. [PubMed: 28686897]

Veneman WJ, Spaink HP, Brun NR, Bosker T, & Vijver MG (2017). Pathway analysis of systemic transcriptome responses to injected polystyrene particles in zebrafish larvae. Aquatic Toxicology, 190, 112–120. doi:10.1016/j.aquatox.2017.06.014 [PubMed: 28704660]

Wallace KN, & Pack M (2003). Unique and conserved aspects of gut development in zebrafish. Developmental biology, 255(1), 12–29. [PubMed: 12618131]

Westerfield M, (2000). The Zebrafish Book: A Guide for the Laboratory Use of Zebrafish (*Danio rerio*). Oregon: University of Oregon Press, 8 p.

Xie J, Farage E, Sugimoto M, & Anand-Apte B (2010). A novel transgenic zebrafish model for blood-brain and blood-retinal barrier development. BMC developmental biology, 10(1), 76. [PubMed: 20653957]

Zhao B, Sun L, Zhang W, Wang Y, Zhu J, Zhu X, & Zhang Y (2014). Secretion of intestinal goblet cells: a novel excretion pathway of nanoparticles. Nanomedicine: Nanotechnology, Biology and Medicine, 10(4), 839–849.

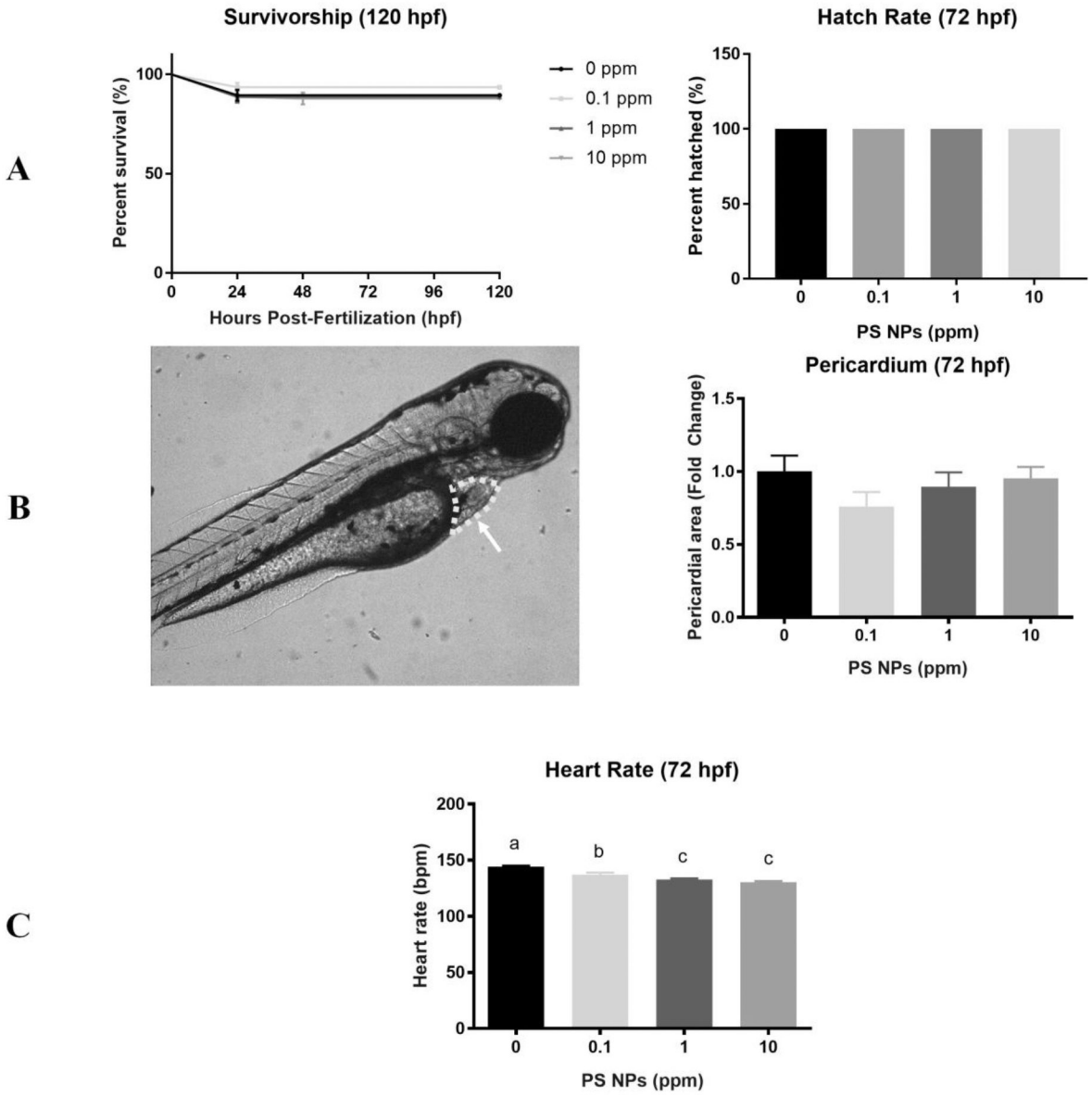

Figure 1. Survivorship, hatch rate, and cardiotoxicity in zebrafish larvae exposed to polystyrene nanoparticles (PS NPs).

(A) Mortality of larvae exposed to PS NPs. Survivorship from 24–120 hpf (n=124–240). Hatch rate was evaluated at 72 hpf (n=50). (B) Pericardial area expressed as fold change. The circled area that the arrow is pointing at in the image is representative of the pericardial area used (n=5). (C) Heart rate in beats per minute (bpm) (n=15). All data are presented as means ± SEM. Significance was accepted if $p<0.05$. Different letters denote statistical differences across treatments.

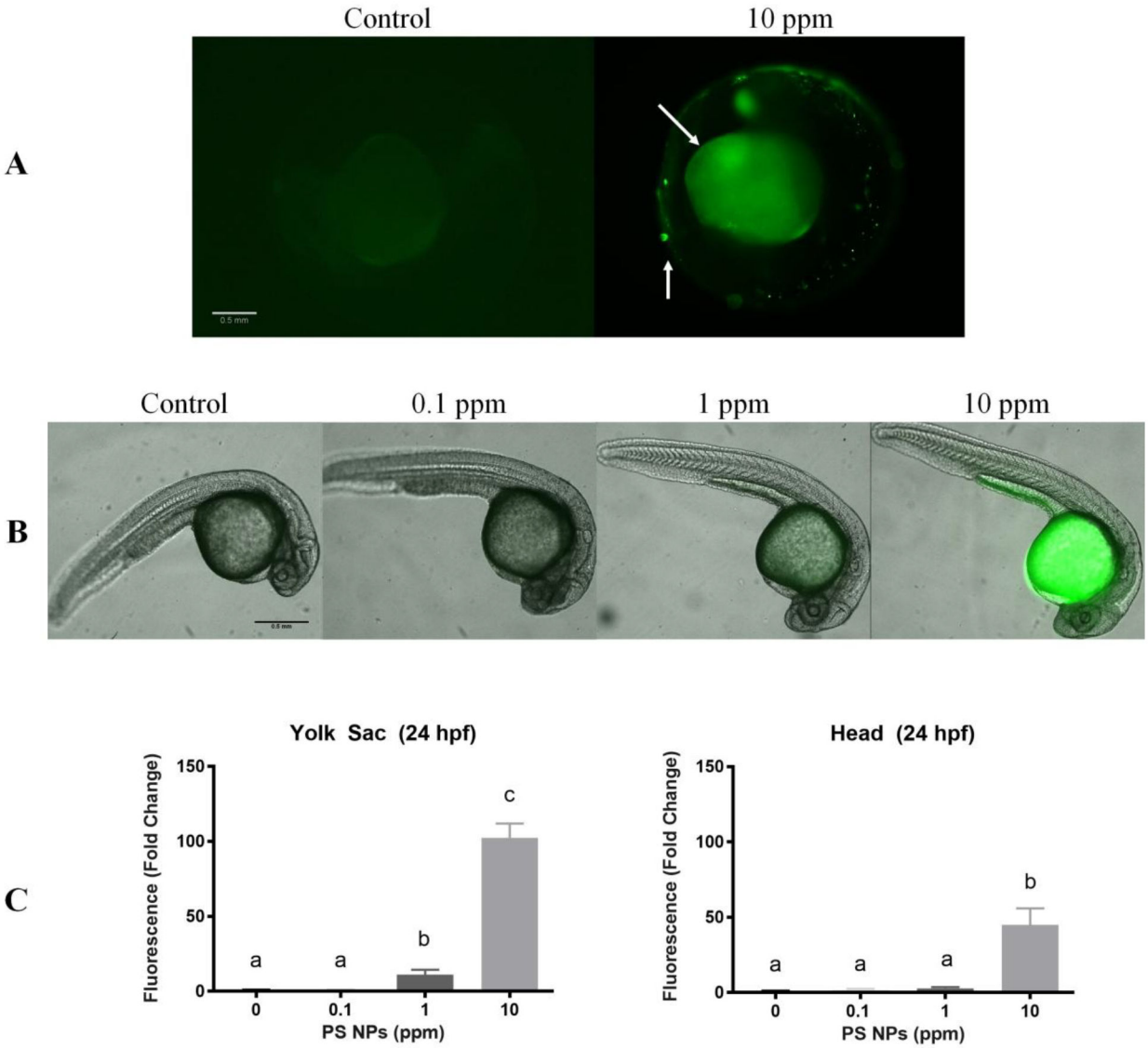

Figure 2. Polystyrene nanoparticles (PS NPs) fluorescence and distribution in 24 hpf zebrafish embryos

PS NPs fluorescence in zebrafish embryos at 24 hpf. Embryos were exposed with the chorion intact but were dechorionated prior to imaging (n=5). (A) Fluorescence in the chorionated zebrafish embryos. The arrows indicate PS NP aggregates on the surface of the chorion and fluorescence in the yolk sac. (B) Fluorescence in zebrafish embryos dechorionated prior to imaging to show PS NPs penetrated the chorion. (C) Fluorescence in the head and yolk sac of zebrafish embryos dechorionated prior to imaging. All fluorescence data are presented as fold change (means ± SEM). Significance was accepted if $p<0.05$. Different letters denote statistical differences across treatments

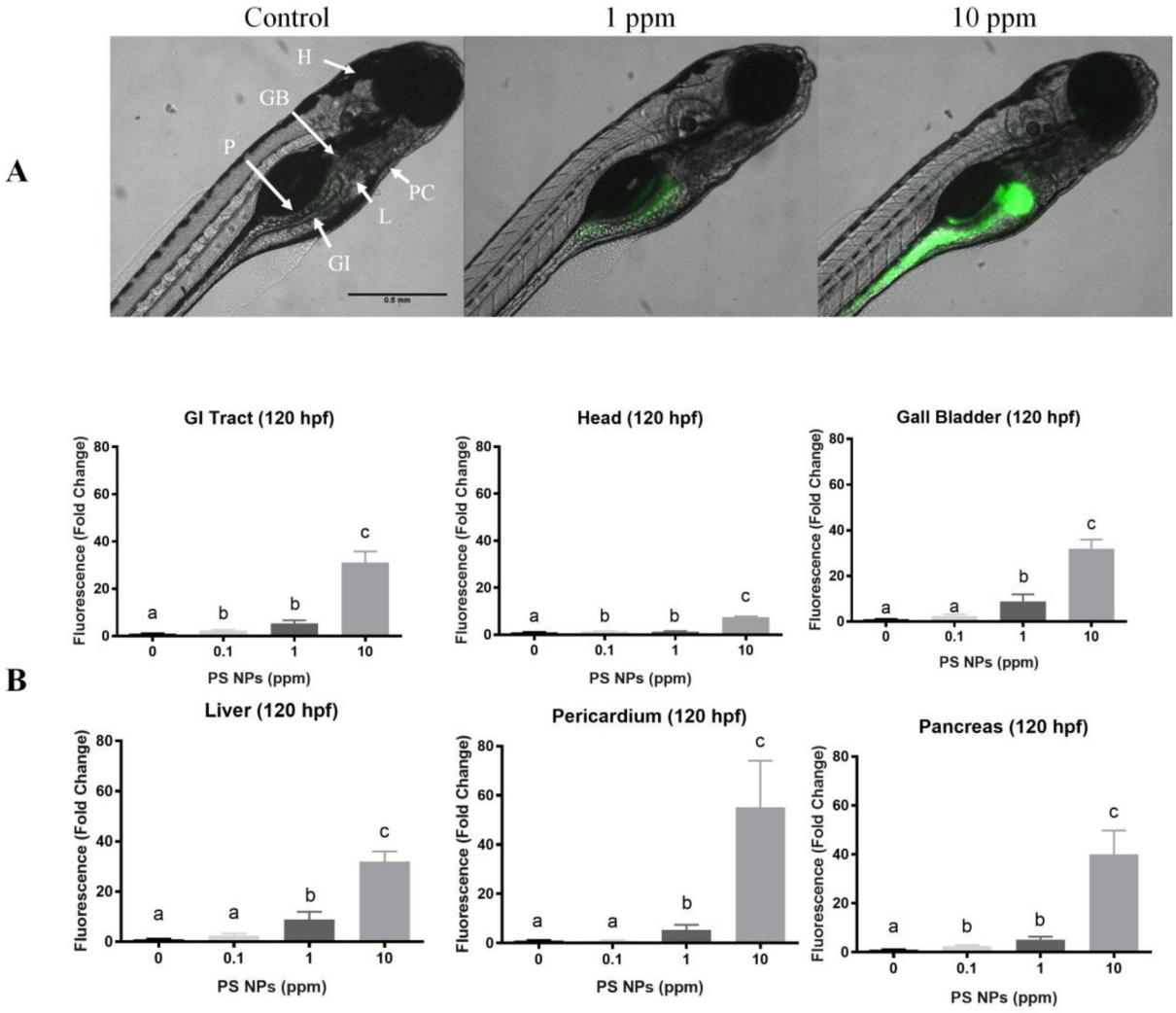

Figure 3. Polystyrene nanoparticles (PS NPs) fluorescence and distribution in 120 hpf zebrafish larvae

PS NPs fluorescence in zebrafish larvae at 120 hpf (n=5). (A) Fluorescence in the zebrafish larvae. The letters in the control image correspond to the various organs analyzed: (H) head, (GB) gall bladder, (P) pancreas, (PC) pericardium, (L) liver, (GI) gastrointestinal tract. (B) Fluorescence in the gastrointestinal tract, head, gall bladder, liver, pericardial area, and pancreas of zebrafish larvae presented as fold change (means ± SEM). Significance was accepted if $p<0.05$. Different letters denote statistical differences across treatments.

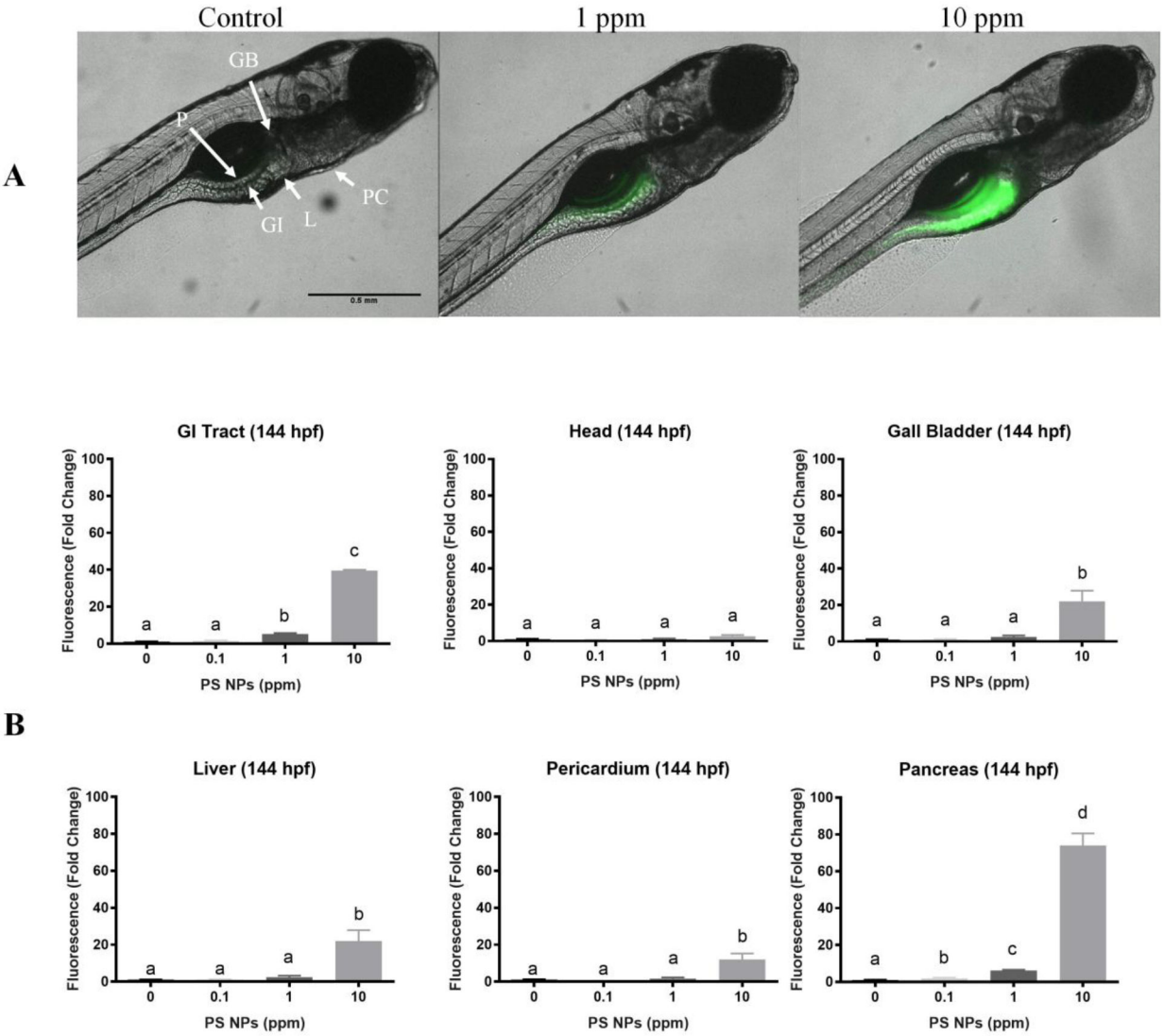

Figure 4. Polystyrene nanoparticles (PS NPs) fluorescence and distribution in 168 hpf zebrafish larvae

PS NPs fluorescence in zebrafish larvae at 168 hpf after 48 h of depuration (n=5). These images represent the last day of recovery. (A) Fluorescence in the zebrafish larvae. The letters in the control image correspond to the various organs analyzed: (H) head, (GB) gall bladder, (P) pancreas, (PC) pericardium, (L) liver, (GI) gastrointestinal tract. (B) Fluorescence of the gastrointestinal tract, head, gall bladder, liver, pericardial area, and pancreas of zebrafish larvae presented as fold change (means ± SEM). Significance was accepted if $p<0.05$. Different letters denote statistical differences across treatments.

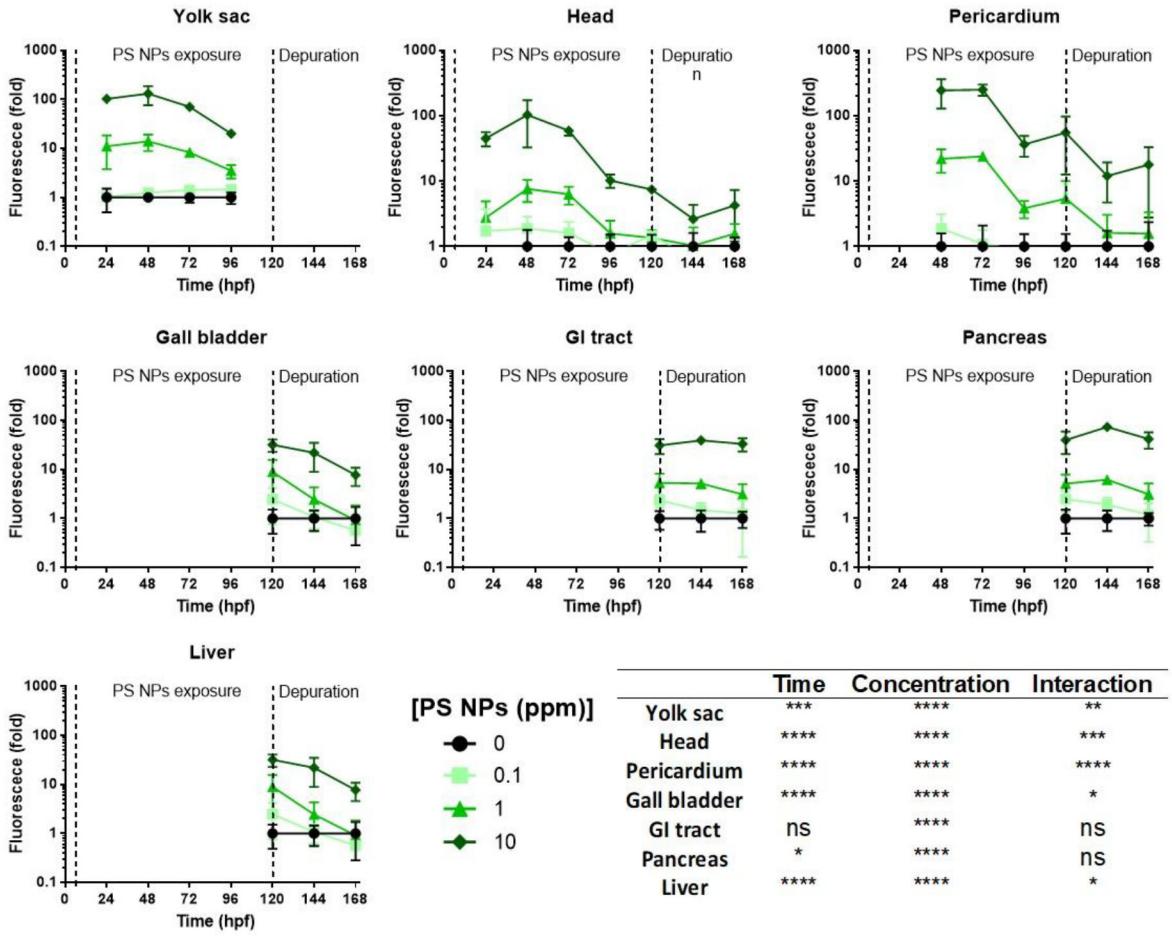

Fig 5. Polystyrene nanoparticles (PS NPs) fluorescence and distribution throughout the zebrafish development.

Green fluorescence in different areas or organs of zebrafish embryos and larvae (n=5). Exposure to PS NPs started at 6 hpf and finished at 120 hpf. At this time point, PS NPs were removed and animals were allowed to depurate until 168 hpf. At 120 hpf, the yolk sac is resorbed, and the gall bladder, gastrointestinal (GI tract), pancreas, and liver are visible. Data are plotted against a logarithmic scale. Two-way ANOVA results are summarized in the bottom right panel, including the p-value for each factor (time of exposure and NP PSs concentration) and their interaction (* $p<0.05$, ** $p<0.01$, *** $p< 0.001$, **** $p<0.0001$, ns $p>0.05$).

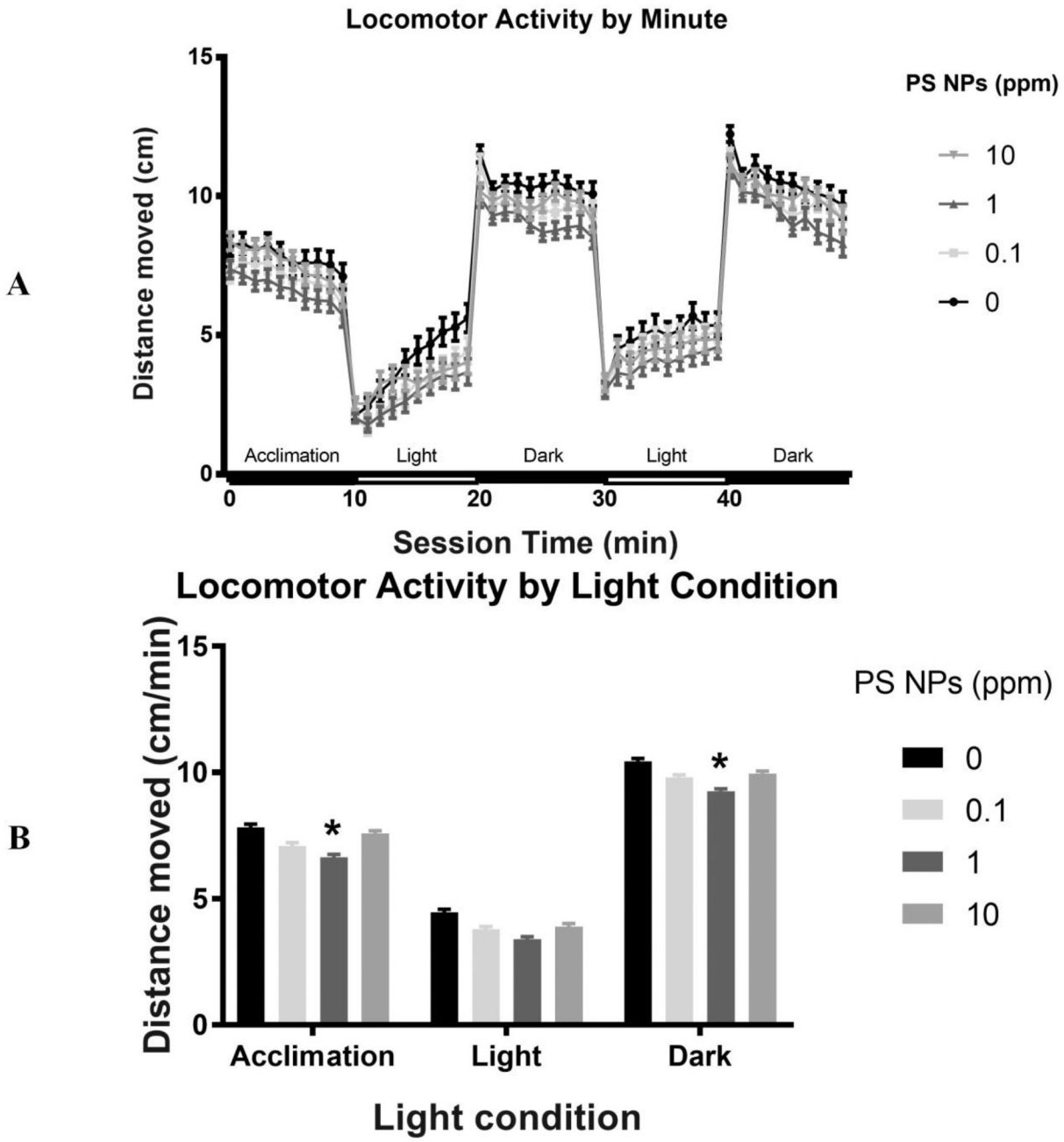

Fig 6. Behavioral toxicity in zebrafish larvae exposed to polystyrene nanoparticles (PS NPs).

(A) Locomotor activity by light condition of larvae (144 hpf) exposed to PS NPs. The above plot represents average distance travelled per minute (cm/min) as a function of light condition (n=70–72). (B) Locomotor activity by light condition of larvae exposed to PS NPs. For both (A) & (B), data are presented as means ± SEM. Significance was accepted if $p<0.05$. * represents significant difference from control within the condition.